

The Angular Momentum Content of Dwarf Galaxies: New Challenges for the Theory of Galaxy Formation

Frank C. van den Bosch¹, Andreas Burkert², and Rob A. Swaters³

¹*Max-Planck Institut für Astrophysik, Karl Schwarzschild Str. 1, Postfach 1317, 85741 Garching, Germany*

²*Max-Planck Institut für Astronomie, Königstuhl 17, D-69117 Heidelberg, Germany*

³*Carnegie Institution of Washington, Washington DC 20015, USA*

ABSTRACT

We compute the specific angular momentum distributions of a sample of low mass disk galaxies observed by Swaters. We compare these distributions to those of dark matter haloes obtained by Bullock et al. from high resolution N -body simulations of structure formation in a Λ CDM Universe. We find that although the disk mass fractions are significantly smaller than the Universal baryon fraction, the total specific angular momenta of the disks are in good agreement with those of dark matter haloes. This suggests that disks form out of only a small fraction of the available baryons, but yet manage to draw most of the available angular momentum. In addition we find that the angular momentum distributions of disks are clearly distinct from those of the dark matter; disks lack predominantly both low and high specific angular momentum. Understanding these findings in terms of a coherent picture for disk formation is challenging. Cooling, feedback and stripping, which are the main mechanisms to explain the small disk mass fractions found, seem unable to simultaneously explain the disk's angular momentum distribution. In fact, it seems that the baryons that make up the disks must have been born out of angular momentum distributions that are clearly distinct from those of Λ CDM haloes. However, the dark and baryonic mass component experience the same tidal forces, and it is therefore expected that they should have similar angular momentum distributions. Therefore, understanding the angular momentum content of disk galaxies remains an important challenge for our picture of galaxy formation.

Key words: galaxies: formation — galaxies: fundamental parameters — galaxies: kinematics and dynamics — galaxies: structure — dark matter.

1 INTRODUCTION

Disk galaxies are rotationally supported systems whose structure is governed by angular momentum. In the current paradigm of structure formation, galaxies form hierarchically by the assembly of dark matter haloes and the subsequent cooling of the baryonic mass component. In this standard picture, protogalaxies acquire angular momentum by tidal interactions with neighboring protogalaxies; the so-called cosmological torques (Hoyle 1953). This mechanism of spinning up the dark and baryonic matter has been studied in great detail using numerical simulations (e.g., Barnes & Efstathiou 1987; Warren et al. 1992; Zurek, Quinn & Salmon 1988; Sugerma, Summers & Kamionkowski 2000) and found to be in good agreement with linear tidal-torque theory (e.g., Doroshkevich 1970; White 1984; Catelan & Theuns 1996).

Following Peebles (1969) it has become customary to

parameterize the angular momentum of dark matter haloes by the dimensionless spin parameter

$$\lambda = \frac{J|E|^{1/2}}{GM^{5/2}} \quad (1)$$

where J , E , and M are the total angular momentum, energy and mass of the halo, and G is the gravitational constant. The distribution of λ is well described by a log-normal distribution,

$$p(\lambda)d\lambda = \frac{1}{\sigma_\lambda\sqrt{2\pi}} \exp\left(-\frac{\ln^2(\lambda/\bar{\lambda})}{2\sigma_\lambda^2}\right) \frac{d\lambda}{\lambda}, \quad (2)$$

with $\bar{\lambda} \simeq 0.06$ and $\sigma_\lambda \simeq 0.5$ (e.g., Barnes & Efstathiou 1987; Ryden 1988; Cole & Lacey 1996; Warren et al. 1992). Starting with the seminal paper of Fall & Efstathiou (1980), it was soon realized that the size distribution of disk galaxies can be explained as originating from the spin parameter distribution if the assumption is made that baryons conserve their specific angular momentum when cooling to form lu-

minous galaxies. This concept has spawned our current picture for the formation of disk galaxies, which has been addressed by numerous studies. Blumenthal et al. (1986) and Flores et al. (1993) investigated how adiabatic contraction of dark matter haloes impacts on the rotation curves of disk galaxies. Kauffmann (1996) linked the formation of disk galaxies within this framework to the evolution of damped Ly α absorption systems. Dalcanton, Spergel & Summers (1997) and Mo, Mao & White (1998) investigated the structural properties of disks, with emphasis on the variance induced by the λ -distribution. Subsequent studies included recipes for bulge formation, gas viscosity, star formation and/or feedback and investigated more detailed properties of these model disk galaxies, such as the Tully-Fisher relation, the gas mass fractions, and the origin of the Hubble sequence (van den Bosch 1998, 2000, 2001; Jimenez et al. 1998; Natarajan 1999; Heavens & Jimenez 1999; van den Bosch & Dalcanton 2000; Firmani & Avila-Reese 2000; Avila-Reese & Firmani 2000; Efstathiou 2000; Zhang & Wyse 2000; Buchalter, Jimenez & Kamionkowski 2001).

The standard picture of disk formation that has emerged from these studies has been remarkably successful in explaining a wide variety of observational properties of disk galaxies. However, two important problems, both related to the angular momentum of disk galaxies, have come to light. First of all, detailed hydro-dynamical simulations of this process of disk formation in a cold dark matter (CDM) Universe yield disks that are an order of magnitude too small (Navarro & Benz 1991; White & Navarro 1993; Steinmetz & Navarro 1999). This problem, known as the angular momentum catastrophe, is a consequence of the hierarchical formation of galaxies which causes the baryons to lose a large fraction of their angular momentum to the dark matter. The second problem concerns the actual density distribution of disk galaxies. Under the assumption of detailed angular momentum conservation, this density distribution is a direct reflection of the distribution of specific angular momentum of the protogalaxy. Although the distribution of *total* specific angular momentum of dark matter haloes is well established (i.e., equation [2]), little is known about the actual distribution of specific angular momentum in each individual halo. Therefore, prompted by the observed surface brightness profiles of disk galaxies, most models for the formation of disk galaxies have made the *a priori* assumption that the disks that form have exponential density distributions. Recently, however, Bullock et al. (2000) determined the angular momentum distributions of individual dark matter haloes, and showed that disks that form out of such distributions are more centrally concentrated than an exponential. Van den Bosch (2001) has shown that when star formation, bulge formation, and feedback are taken into account, the resulting stellar density distributions are inconsistent with observations, at least for the low surface brightness disk galaxies. In addition, van den Bosch showed that the truncation radii of the resulting disks are too small compared to observations.

From the above discussion it is clear that our understanding of the formation of disk galaxies is directly related to the angular momentum distribution (hereafter AMD) of the baryonic mass component of protogalaxies. In this paper we use the observed density distributions and rotation curves of a sample of 14 dwarf galaxies to compute their

AMDs. A comparison of these AMDs with those of dark matter haloes then provides important clues to the formation process of disk galaxies.

This paper is organized as follows. In Section 2 we discuss the angular momentum distributions expected on grounds of the standard paradigm of galaxy formation. In Section 3 we then present the angular momentum distributions of a sample of 14 dwarf galaxies. The implications of these distributions for our picture of galaxy formation are discussed in Section 4, and we summarize our results in Section 5.

Whenever the cosmological framework is important for our discussion we adhere to the currently popular Λ CDM model with $\Omega_0 = 0.3$, $\Omega_\Lambda = 0.7$, $h = 0.7$, and $\sigma_8 = 1.0$. This model yields a reasonable fit to the current suite of cosmological constraints, including high redshift supernovae (Perlmutter et al. 1998; Riess et al. 1998; Garnavich et al. 1998), the cosmic microwave background radiation (e.g., de Bernardis et al. 2000), and the observed cluster abundances (Eke, Cole & Frenk 1996; Bahcall & Fan 1998). For the baryon density we adopt $\Omega_{\text{bar}} = 0.019 h^{-2}$ as suggested by the observations of primordial deuterium abundances by Tytler et al. (1999). With the cosmological parameters defined as above this implies a Universal baryonic mass fraction of $f_{\text{bar}} = \Omega_{\text{bar}}/\Omega_0 = 0.13$.

2 THEORETICAL BACKGROUND

Consider a virialized halo with mass M_{vir} consisting of dark and baryonic matter, and let $p(j)dj$ indicate the fraction of mass with specific angular momentum between j and $j+dj$. The total specific angular momentum is given by

$$j_{\text{tot}} = j_{\text{max}} \left[1 - \int_0^1 m(l)dl \right] \equiv \zeta j_{\text{max}}. \quad (3)$$

Here j_{max} is the maximum specific angular momentum of $p(j)$, $l = j/j_{\text{max}}$, and $m(j)$ is the normalized cumulative distribution

$$m(j) = \int_0^j p(j)dj. \quad (4)$$

The dimensionless spin parameter λ can be related to j_{tot} as

$$\lambda = \frac{j_{\text{tot}}}{\sqrt{2} r_{\text{vir}} V_{\text{vir}}} \mathcal{G}. \quad (5)$$

Here r_{vir} is the virial radius, $V_{\text{vir}} = \sqrt{GM_{\text{vir}}/r_{\text{vir}}}$, and \mathcal{G} is a geometrical factor.

It is customary to parameterize the density distribution of virialized structures as

$$\rho_{\text{vir}}(r) = \rho_s \left(\frac{r}{r_s} \right)^{-\gamma} \left(1 + \frac{r}{r_s} \right)^{\gamma-3} \quad (6)$$

with r_s a scale-length and $\rho_s = \rho_{\text{vir}}(r_s)$. For the density distribution of the form (6), which reduces to the NFW profile (Navarro, Frenk & White 1996, 1997) for $\gamma = 1.0$, one finds

$$\mathcal{G} = \mathcal{G}(\gamma, c_{\text{vir}}) = \sqrt{h(c_{\text{vir}})} f^{-1}(c_{\text{vir}}), \quad (7)$$

where $c_{\text{vir}} = r_{\text{vir}}/r_s$ is the halo concentration parameter,

$$f(x) = \int_0^x dy y^{2-\gamma} (1+y)^{\gamma-3}, \quad (8)$$

and

$$h(x) = x \int_0^x dy f(y) y^{1-\gamma} (1+y)^{\gamma-3}. \quad (9)$$

In the standard picture of disk formation it is assumed that baryonic and dark matter experience the same tidal torques, and thus end up with the same AMD $p(j)$. As shown by Bullock et al. (2000, hereafter B00) the AMD of dark matter haloes is well described by

$$m(l) = \frac{\mu l}{l + \mu - 1}, \quad (10)$$

with $l = j/j_{\max}$. For dark matter haloes in a Λ CDM Universe with $\Omega_0 = 0.3$, $\Omega_\Lambda = 0.7$, $h = 0.7$, and $\sigma_8 = 1.0$, B00 found that the distribution of μ is Gaussian in $\log(\mu - 1)$ with a mean of -0.6 and a standard deviation of 0.4 . Thus for 90 percent of the haloes $1.06 < \mu < 2.0$ with a mean of $\langle \mu \rangle = 1.25$. For the probability distribution corresponding to (10) one can write

$$p(s) = \frac{\zeta \mu (\mu - 1)}{(\zeta s + \mu - 1)^2}, \quad (11)$$

with $s = j/j_{\text{tot}}$ and

$$\zeta = \frac{j_{\text{tot}}}{j_{\max}} = 1 - \mu \left[1 - (\mu - 1) \ln \left(\frac{\mu}{\mu - 1} \right) \right]. \quad (12)$$

If our current picture for the formation of disk galaxies is correct, the baryonic mass of disk galaxies thus should have an AMD of the form (11). However, not necessarily all the baryons inside r_{vir} are currently part of the disk (stars plus cold gas). Part of the baryons may not have cooled by the present time, and/or a certain fraction of the baryons may have been expelled from the halo by either feedback processes (i.e., galactic winds) or by some stripping mechanism. We therefore define the fraction $f_{\text{disk}} = M_{\text{disk}}/M_{\text{vir}}$, where M_{disk} is the total disk mass observed. If all available baryons have cooled to become part of the disk one expects that $f_{\text{disk}} = f_{\text{bar}}$. By comparing the AMD of the observed disk with that of equation (11), and by investigating how these AMDs correlate with f_{disk} , important insights into the formation mechanism of dwarf galaxies can be obtained.

3 THE ANGULAR MOMENTUM CONTENT OF DWARF GALAXIES

3.1 Description of the data

In order to compute the angular momentum distribution of the baryonic component of a disk galaxy one needs (i) the rotation velocity as function of radius, (ii) the distribution of the stellar mass, and (iii) the distribution of the gas. One thus requires a combination of both optical and HI observations. Since most angular momentum is contained by material at large galactocentric radii it is essential that the observations probe out to large enough radii. Recently, Swaters (1999) obtained both optical (R -band) and HI observations of a large sample of dwarf galaxies, down to fairly low HI surface brightness. These data are therefore ideally suited to compute angular momentum distributions. A subset of these data, with the highest quality rotation curves, was analyzed in detail by van den Bosch & Swaters (2001; hereafter BS01).

Table 1. Properties of sample of late-type dwarf galaxies.

UGC	D	M_R	μ_0^R	R_d	V_{last}	i
731	8.0	-16.63	23.0	1.65	74	57
3371	12.8	-17.74	23.3	3.09	86	49
4325	10.1	-18.10	21.6	1.63	92	41
4499	13.0	-17.78	21.5	1.49	74	50
6446	12.0	-18.35	21.4	1.87	80	52
7399	8.4	-17.12	20.7	0.79	109	55
7524	3.5	-18.14	22.2	2.58	79	46
8490	4.9	-17.28	20.5	0.66	78	50
9211	12.6	-16.21	22.6	1.32	65	44
11707	15.9	-18.60	23.1	4.30	100	68
11861	25.1	-20.79	21.4	6.06	153	50
12060	15.7	-17.95	21.6	1.76	74	40
12632	6.9	-17.14	23.5	2.57	76	46
12732	13.2	-18.01	22.4	2.21	98	39

Column (1) lists the UGC number of the galaxy. Columns (2) – (7) list the distance to the galaxy (in Mpc), absolute R -band magnitude, central R -band surface brightness (in mag arcsec $^{-2}$), scale length of the stellar disk (in kpc), the observed rotation velocity V_{last} (in km s $^{-1}$) at the last measured point, and the adopted inclination angle (in degrees), respectively. Magnitudes and central surface brightnesses have been corrected for inclination and galactic extinction, but not for internal extinction.

Taking account of the effects of beam smearing and adiabatic contraction they determined the concentration and the virial velocities of the dark matter haloes, which they found to be consistent with predictions of Λ CDM models. In the following we concentrate on the 14 galaxies for which BS01 achieved a meaningful fit. These galaxies are listed in Table 1, together with some global properties taken from Swaters (1999).

3.2 Mass modeling

We now turn to computing the angular momentum distributions of the 14 dwarf galaxies in our sample. For that purpose we first construct a mass model of each galaxy that best fits the observed rotation curve after the effects of beam smearing are taken into account. If the effects of beam smearing are small, one could in principle directly infer the angular momentum distribution from the observed $V_{\text{rot}}(r)$ and the surface density distributions of the stars and gas. However, the advantage of the mass modeling is that typically HI is measured out to much larger radii than the maximum radius out to which V_{rot} is determined (simply because a measurement of Σ_{HI} requires a lower S/N than V_{rot}). Since low surface brightness HI at large radii can still contain a significant fraction of the total mass, and has high specific angular momentum, it is essential that one takes this gas into account. A proper mass model that fits the observed rotation curve makes predictions for the circular velocity at all radii, and can thus be used to compute a more complete angular momentum distribution. Furthermore, the mass modeling allows to correct for the effects of beam smearing.

For our mass modeling we use the same method as employed in BS01, which we briefly repeat here for completeness. We assume that there are three mass components in each galaxy: an infinitesimally thin gas disk, a thick stellar disk, and a spherical dark matter halo.

We make the assumption that the gas is distributed

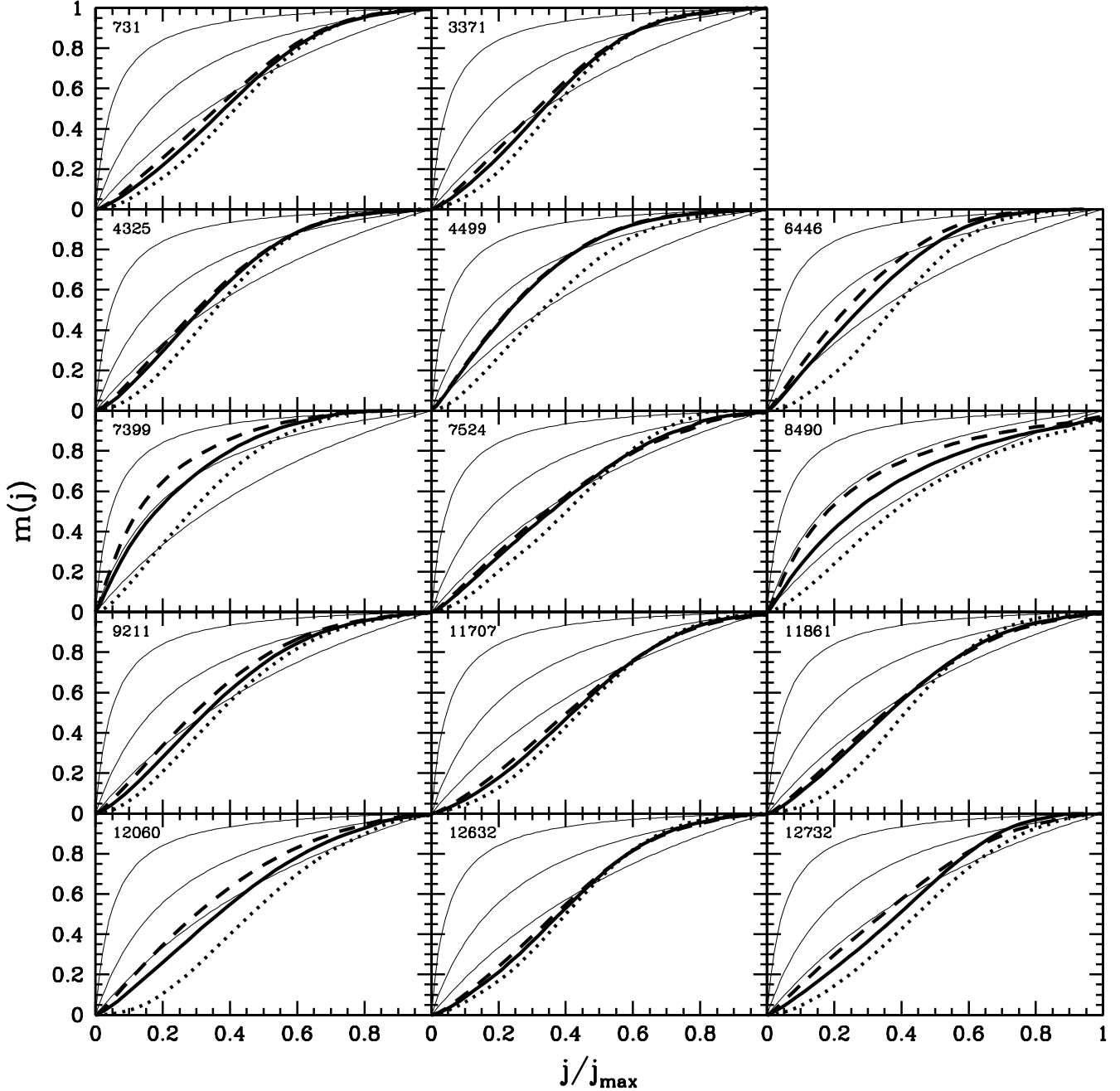


Figure 1. The normalized cumulative angular momentum distribution, $m(j)$, as function of j/j_{\max} . Each panel plots, with thick lines, three distributions for a particular sample galaxy (as indicated in the panel) that correspond to three different values of the stellar mass-to-light ratio: $\Upsilon_R = 0$ (dotted lines), $\Upsilon_R = 1.0$ (M/L_{\odot}) (solid lines), and $\Upsilon_R = 2.0$ (M/L_{\odot}) (dashed lines). The three thin lines correspond to AMDs of the form (10) with $\mu = 1.06$ (upper curves), $\mu = 1.25$ (middle curves) and $\mu = 2.0$ (lower curves) and are plotted for comparison. These values of μ correspond to the mean and the 90 percent range of the distribution in μ found by Bullock et al. (2000) for Λ CDM haloes. Note that the majority of the disks has an AMD that is clearly distinct from that of the dark matter.

axisymmetrically in an infinitesimally thin disk, and model the HI density distribution as:

$$\Sigma_{\text{HI}}(R) = \Sigma_0 \left(\frac{R}{R_1}\right)^{\beta} e^{-R/R_1} + f \Sigma_0 e^{-((R-R_2)/\sigma)^2}. \quad (13)$$

The first term represents an exponential disk with scale length R_1 and with a central hole, the extent of which depends on β . The second term corresponds to a Gaussian ring with radius R_2 and a FWHM $\propto \sigma$. The flux ratio between

these two components is set by f . The form of equation (13) has no particular physical motivation, but is an appropriate fitting function, which yields excellent fits to the observed HI surface brightness distributions (see BS01)*. When com-

* In the case of UGC 7524 the fitting function of equation (13) can not satisfactorily describe the data and linear interpolation between the data points is used to describe $\Sigma_{\text{HI}}(R)$.

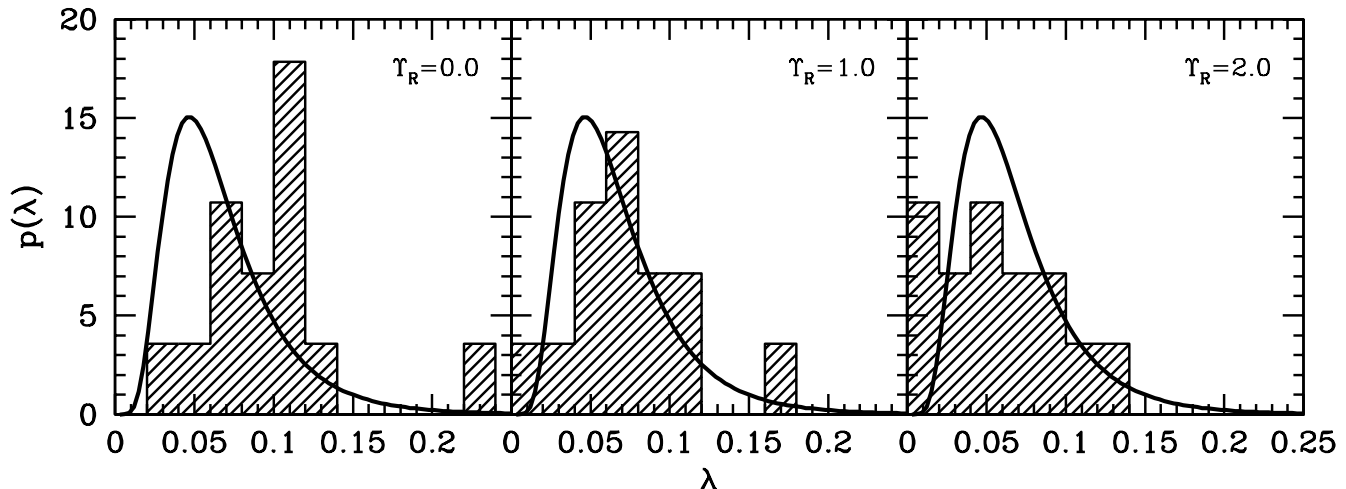


Figure 2. Histograms (hatched) of the distribution of λ_{disk} for the 14 dwarf galaxies in our sample. These values have been determined from the AMDs plotted in Figure 1 using equations (3) and (17). Results are plotted for three values of the stellar mass-to-light ratio, as indicated in each panel. The thick solid lines plots the probability distribution of equation (2) with $\bar{\lambda} = 0.06$ and $\sigma_{\lambda} = 0.5$, and is to represent the spin parameter distribution of dark matter haloes. Especially for $\Upsilon_R = 1.0 (M/L)_{\odot}$ the two distributions agree remarkably well, suggesting that the disks have the same distribution of total specific angular momentum as the dark matter haloes.

Table 2. Results for $\Upsilon_R = 1.0 (M/L)_{\odot}$ and $\gamma = 1.0$.

UGC	c_{vir}	V_{vir}	f_{disk}	f_{gas}	λ_{disk}	j_{tot}	j_{max}
731	17.6	48.6	0.024	0.801	0.061	308	775
3371	10.6	65.5	0.018	0.715	0.056	569	1618
4325	33.0	48.6	0.037	0.541	0.074	328	971
4499	2.4	126.3	0.003	0.672	0.007	330	1195
6446	9.1	56.2	0.041	0.570	0.052	397	1325
7399	19.9	65.8	0.012	0.691	0.044	396	1692
7524	6.4	78.8	0.012	0.500	0.025	393	1025
8490	17.5	53.2	0.026	0.769	0.062	378	1106
9211	19.2	41.2	0.055	0.865	0.107	381	1058
11707	14.6	62.2	0.062	0.770	0.103	886	2046
11861	16.4	93.1	0.068	0.405	0.099	1861	4820
12060	31.1	42.8	0.102	0.710	0.168	582	1477
12632	16.5	47.8	0.033	0.760	0.078	387	976
12732	9.0	68.9	0.040	0.869	0.081	926	2267

Column (1) lists the UGC number of the galaxy. Columns (2) and (3) list c_{vir} and V_{vir} (in km s^{-1}) of the best-fit mass model, respectively. Columns (4) and (5) list the disk mass fraction f_{disk} and the gas mass fraction f_{gas} , respectively. Column (6) lists the baryonic spin parameter λ_{disk} , and columns (7) and (8), list the total and maximum specific angular momentum of the baryons (both in kpc km s^{-1}).

putting the circular velocities of the gas, we multiply Σ_{HI} by a factor 1.3 to correct for the contribution of Helium.

For the stellar disk we assume a thick exponential

$$\rho^*(R, z) = \rho_0^* \exp(-R/R_d) \text{sech}^2(z/z_0) \quad (14)$$

where R_d is the scale length of the disk in the R -band. Throughout we set $z_0 = R_d/6$. The exact value of this ratio, however, does not significantly influence the results. None of the galaxies in our sample has a significant bulge component.

For the DM component we consider a density distribution of the form (6). Unless stated otherwise we focus on haloes with $\gamma = 1.0$ (i.e., NFW profiles). Rather than parameterizing the DM halo by (c_{200}, V_{200}) , as in BS01, we use $(c_{\text{vir}}, V_{\text{vir}})$. Here

$$c_{\text{vir}} = \frac{r_{\text{vir}}}{r_s} = c_{200} \left(\frac{\Delta_{\text{vir}}}{200} \right)^{-1/3}, \quad (15)$$

with Δ_{vir} the virial density, defined as the average density inside r_{vir} expressed in terms of the critical density for closure. For the Λ CDM cosmology used here $\Delta_{\text{vir}} \simeq 101$ (e.g., Bryan & Norman 1998).

When fitting the rotation curves we take adiabatic contraction (Barnes & White 1984; Blumenthal et al. 1986; Flores et al. 1993) and beam smearing into account (see BS01 for details). The best fit values for c_{vir} and V_{vir} are listed in Table 2 together with the inferred values for f_{disk} and f_{gas} . Note that the values of c_{vir} and V_{vir} differ somewhat from the values of c and V_{200} quoted in BS01 owing to the different definitions.

3.3 Angular momentum distributions

After finding the mass model that best fits the observed $\Sigma_{\text{HI}}(r)$ and $V_{\text{rot}}(r)$ we determine $V_c(r)$, $L(r)$, and $M_{\text{HI}}(r)$ on a linear radial grid between $r = 0$ and $r = r_{\text{max}}$. Here $V_c(r)$ is the total circular velocity at r of the best fit model, $L(r)$ is the total R -band luminosity inside r , as computed from the thick exponential, $M_{\text{HI}}(r)$ is the total HI mass inside r computed from the best fit HI surface density distribution, and r_{max} is the maximum radius out to which HI is detected. We define the total disk mass inside radius r as

$$M_{\text{disk}}(r) = \Upsilon_R \cdot L(r) + 1.3 \cdot M_{\text{HI}}(r). \quad (16)$$

We thus assume that the stellar mass-to-light ratio is constant with radius, and that the total gas mass is simply 1.3 times the HI mass to take account of Helium. Any contribution from molecular and/or ionized gas is therefore considered negligible. The distribution of specific angular momentum is simply given by $m(j) = M_{\text{disk}}(r)/M_{\text{disk}}(r_{\text{max}})$ with $j = r V_c(r)$.

In Figure 1 we plot $m(j)$ as function of j/j_{max} for all the galaxies in our sample. Results are shown for three different

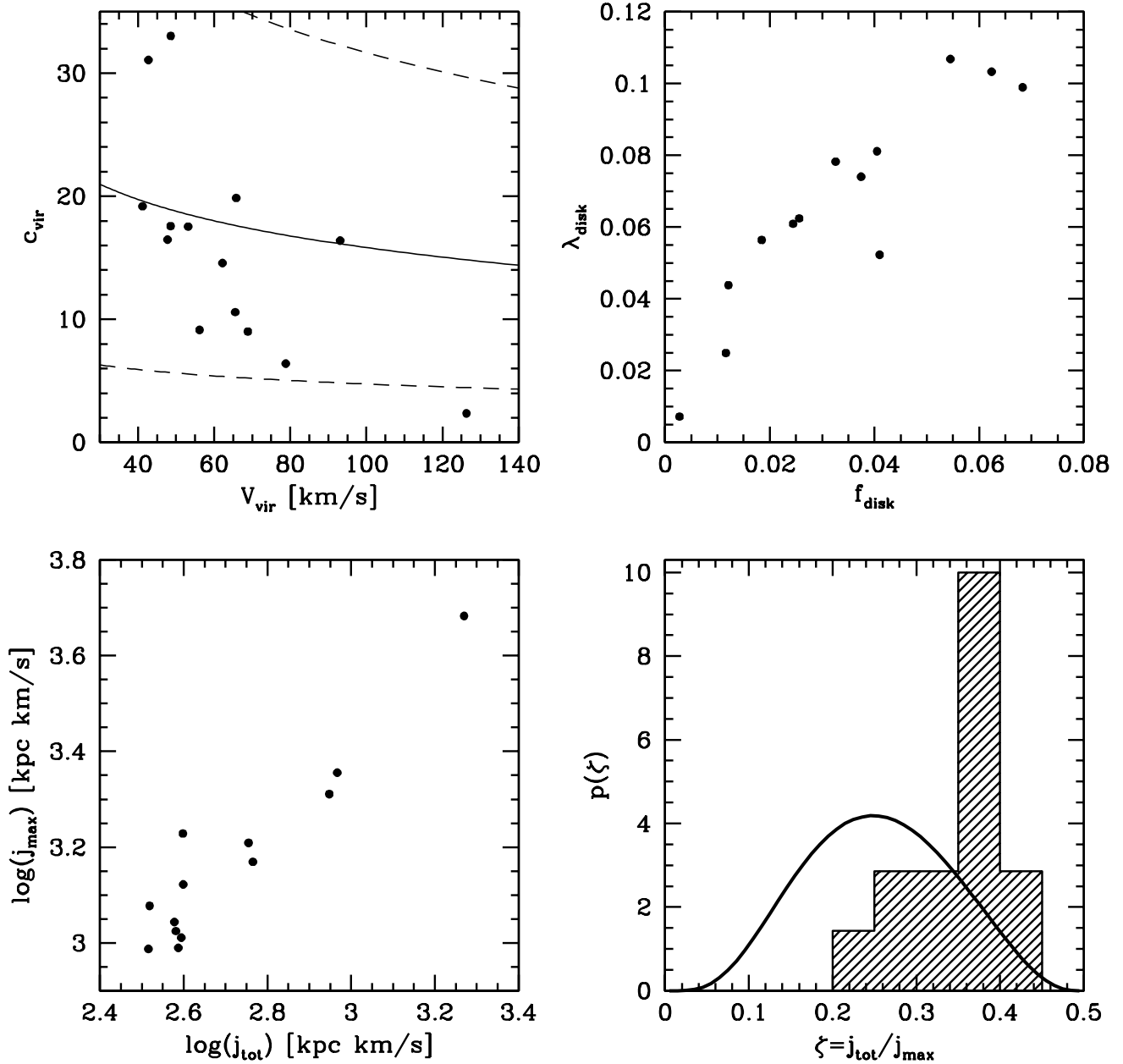


Figure 3. The upper left panel plots c_{vir} versus V_{vir} for the mass models with $\Upsilon_R = 1.0 (M/L)_\odot$ that best fit the observed rotation curves. The solid and dashed lines correspond to the median and 2σ limits of the distribution of c_{vir} for the Λ CDM cosmology adopted here (computed using the model of Bullock et al. 2001). Although the dwarf galaxies reveal a somewhat steeper decline of c_{vir} with increasing V_{vir} , reflecting the degeneracies in the rotation curve fitting, the overall distribution of halo concentrations is in reasonable agreement with the Λ CDM cosmology (see BS01 for a more detailed discussion). The upper right panel reveals a narrow correlation between λ_{bar} (determined from the AMDs) and f_{bar} (inferred from the best fit mass models). The implications of this correlation for the formation of disk galaxies are discussed in detail in the text. The lower left panel plots $\log(j_{\text{max}})$ of the disk versus $\log(j_{\text{tot}})$. The strong correlation found implies a narrow distribution of $\zeta = j_{\text{tot}}/j_{\text{max}}$, which is shown in the lower right panel (shaded histogram). The thick solid curve corresponds to the distribution of ζ of dark matter haloes in a Λ CDM cosmology, and is broader and offset to lower values of ζ . This reiterates that the AMDs of the disks in our sample are different from the AMDs of dark matter haloes found by B00 (see also Figures 1 and 4).

values of the R -band mass-to-light ratio: $\Upsilon_R = 0$ (dotted lines), $\Upsilon_R = 1.0 (M/L)_\odot$ (solid lines), and $\Upsilon_R = 2.0 (M/L)_\odot$ (dashed lines). For comparison, we also plot the specific angular momentum distribution of equation (10) for three values of μ : 1.06, 1.25, and 2.0 (thin solid lines). These distributions outline the 90 percent interval of the AMDs of

Λ CDM haloes (see Section 2). As is immediately apparent, the AMDs of the disks are clearly different from those of Λ CDM haloes.

From the AMDs thus obtained we compute the total specific angular momentum of the disk, j_{tot} , (using equation [3]), which we parameterize by

Table 3. Correlation matrix.

	j_{tot}	j_{max}	f_{disk}	f_{gas}	V_{vir}	c_{vir}
λ_{disk}	0.398	0.231	0.886	0.407	-0.543	0.464
j_{tot}	...	0.886	0.538	-0.055	0.332	-0.262
j_{max}	0.363	-0.024	0.516	-0.270
f_{disk}	0.134	-0.411	0.345
f_{gas}	-0.446	-0.099
V_{vir}	-0.701

Matrix of Spearman Rank's correlation coefficients, r_s , for various parameters of the dwarf galaxies in our sample. A value of $r_s = +1.0$ (-1.0) indicates a perfect correlation (anti-correlation), whereas values of r_s near zero indicate that the parameters are uncorrelated. The only three significant correlations are those between $(\lambda_{\text{disk}}, f_{\text{disk}})$, $(j_{\text{tot}}, j_{\text{max}})$, and $(V_{\text{vir}}, c_{\text{vir}})$. For all other sets of parameters the values of r_s obtained are consistent with no correlation.

$$\lambda_{\text{disk}} = \frac{j_{\text{tot}}}{\sqrt{2} r_{\text{vir}} V_{\text{vir}}} \mathcal{G}(1.0, c_{\text{vir}}). \quad (17)$$

The values of j_{tot} and λ_{disk} are listed in Table 2. In Figure 2 we plot histograms of the normalized probability distributions of λ_{disk} for all three values of Υ_R . For comparison the probability distribution of equation (2) with $\bar{\lambda} = 0.06$ and $\sigma_\lambda = 0.5$ is plotted as thick solid lines. As can be seen, the spin parameter distributions of the disks are fairly similar to that of the dark matter haloes, especially for realistic mass-to-light ratios in the range $1.0 (M/L)_\odot \lesssim \Upsilon_R \lesssim 2.0 (M/L)_\odot$. This implies that, on average, the *total* specific angular momentum of the disks is similar to that of the dark matter. Yet, as we have seen from Figure 1, their *distributions* of specific angular momentum are clearly distinct from that of the dark matter haloes. Furthermore, the baryonic mass fractions inferred from the best fit models to the observed rotation curves are significantly smaller than the Universal value f_{bar} . All this holds important clues to the formation of (dwarf) galaxies, which we discuss in the next section.

4 THE FORMATION OF DWARF GALAXIES

In what follows we restrict ourselves to the AMDs for $\Upsilon_R = 1.0 (M/L)_\odot$, which is a realistic value for the stellar mass-to-light ratio given the typical colors of the dwarfs in our sample (BS01; Bell & de Jong 2001). As we address shortly in Section 4.3 below, none of our results are sensitive to this particular value of Υ_R .

4.1 Clues from parameter correlations

In order to assess whether any significant correlations exist among the various parameters listed in Table 2 we compute the Spearman rank coefficients r_s . The resulting correlation matrix is listed in Table 3. The only significant correlations are those between V_{vir} and c_{vir} (the probability of obtaining $r_s = -0.701$ under the null hypothesis that no correlation exists is $p_s = 5.2 \times 10^{-3}$), and between λ_{disk} and f_{disk} , and j_{max} and j_{tot} (both with $r_s = 0.886$ and $p_s = 2.5 \times 10^{-5}$). We now address the meaning of each of these three correlations, which are plotted in Figure 3.

The decrease of c_{vir} with increasing V_{vir} is, to first order, consistent with what one expects for a Λ CDM cosmology. This is indicated by the solid and dashed lines in the upper

right panel of Figure 3, which correspond to the mean and the 2σ limits of the distribution of halo concentrations as predicted by the Bullock et al. (2001) model for the Λ CDM cosmology adopted here. However, given the amount of scatter expected, it is surprising that we find such a strong anti-correlation; i.e., the slope of the relation between V_{vir} and c_{vir} of the dwarf galaxies in our sample seems too steep. This most likely reflects degeneracies in the rotation curve fitting: a small under-(over)estimate of V_{vir} can result in a relatively large over-(under)estimate of c_{vir} (see BS01 for a more detailed discussion).

The strong correlation between j_{tot} and j_{max} signals a small dispersion in the distribution of ζ . This is shown in the lower right panel of Figure 3. The hatched histogram corresponds to the distribution in ζ for the 14 dwarf galaxies in our sample. We can compare this to the ζ -distribution expected for dark matter haloes by converting the distribution in μ found by B00 using the correspondence between μ and ζ (equation [12]). The resulting probability distribution $p(\zeta)$ is plotted as a thick solid line. Comparing $p(\zeta)$ of the dark matter haloes with that of the dwarf galaxies one notes two important differences. First of all, the latter is significantly narrower than the former (which explains the strong correlation between j_{tot} and j_{max}). Secondly, the mean ζ of the dwarf galaxies is larger than that of the dark matter haloes. Low values of ζ imply AMDs with a long tail to high specific angular momentum, and such AMDs are apparently underrepresented in disk galaxies compared to dark matter haloes (but see Section 4.3.2 below).

The correlation between λ_{disk} and f_{disk} , in the sense that dwarf galaxies with a higher inferred disk mass fraction have a higher specific angular momentum, is remarkably strong. Based on the same set of data, but using a less detailed computation of λ_{disk} based on the stellar component only, a similarly strong correlation between λ_{disk} and f_{disk} was recently found by Burkert (2000b). At first sight such correlation is consistent with an inside-out formation scenario: the baryons that make up stars and cold gas have cooled from the inside out to form the galaxies. Since most angular momentum is contained in the outermost mass shells, which cool latest, one thus expects a correlation as seen. However, the problem with this interpretation is that if only a small fraction of the baryons have cooled, one would expect the total specific angular momentum of the disks to be significantly smaller than that of the dark matter. Yet, the distribution of λ_{disk} is comparable to that of dark matter haloes, whereas f_{disk} is significantly smaller than f_{bar} . Apparently, galactic disks in low-mass systems form only out of a small fraction of the total baryonic mass, but yet manage to draw most of the available angular momentum. This puzzling aspect has recently also been noted by Navarro & Steinmetz (2000), using simple scaling relations of disk galaxies.

4.2 Challenges for the standard model of disk formation

In the standard picture, disks form out of baryons that cool and conserve their specific angular momentum. Since both baryons and dark matter experience the same tidal forces, it is generally assumed that both have the same angular momentum distribution. Therefore, initially the AMD of the

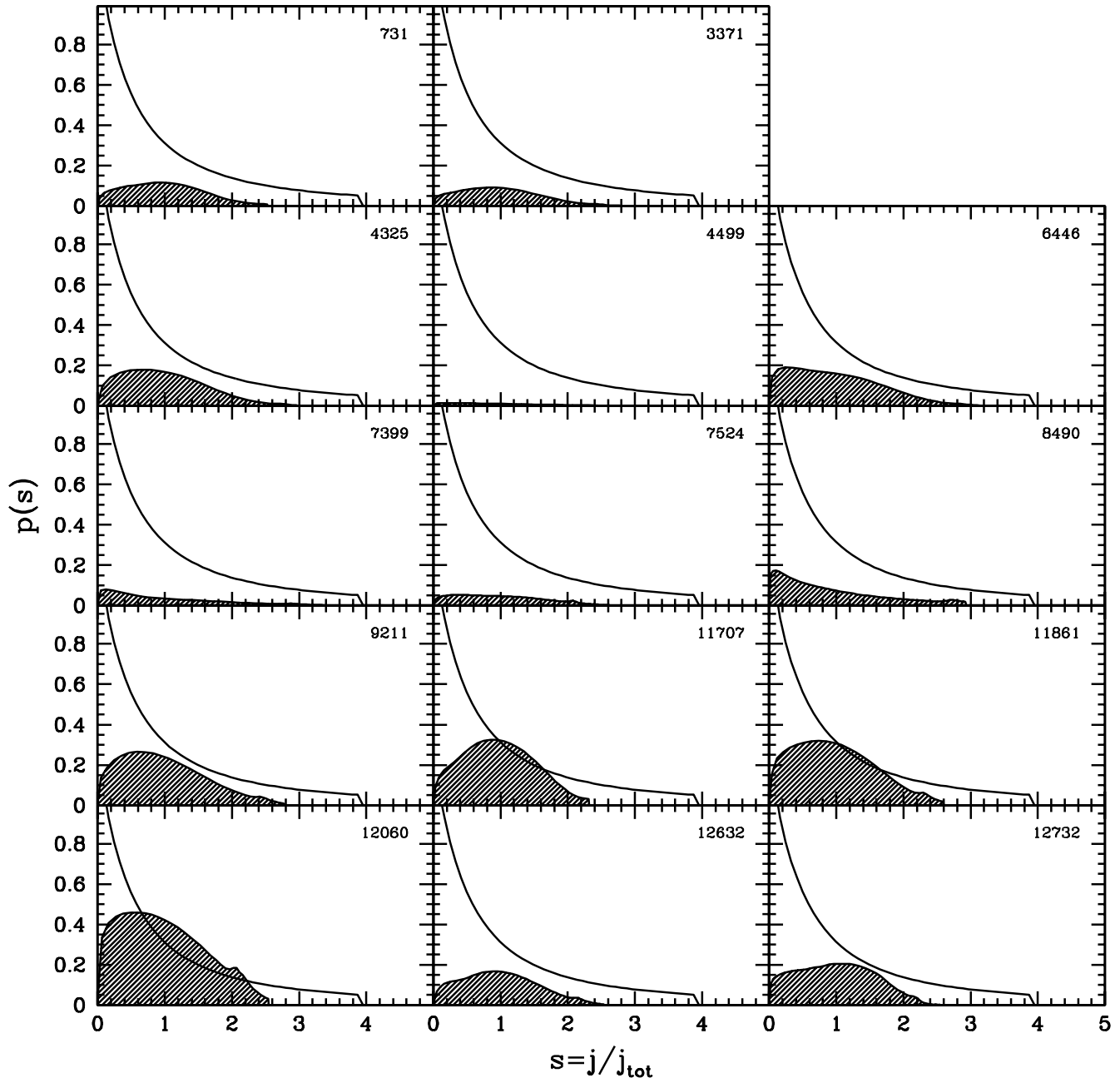


Figure 4. The shaded areas indicate the AMDs $p(s)$ of the 14 disk galaxies in our sample, normalized to $f_{\text{disk}}/f_{\text{bar}}$. For comparison we plot $p(s)$ of equation (11) with $\mu = 1.25$ (normalized to unity), and which represents the median of the AMDs of Λ CDM haloes. Under the standard assumption that baryons conserve their specific angular momentum the difference between the two distributions reflects the AMD of the baryonic matter that is not incorporated in the disk. Note that it is preferentially the baryonic matter with both the highest and the lowest angular momentum that is absent in the disks.

baryonic component, with mass $f_{\text{bar}}M_{\text{vir}}$, can be parameterized by equation (11). A comparison of this distribution with the probability distributions $p(s)$ of real galaxies can be used to test this standard picture and/or provide useful insights regarding the details of galaxy formation. Such comparison is only valid if the total baryonic mass and the disk material have the same j_{tot} (after all $s = j/j_{\text{tot}}$). The fact that the distribution of λ_{disk} for our sample of dwarf galaxies is consistent with $p(\lambda)$ of dark matter haloes (cf.

Figure 2) shows that this is a valid assumption to make, at least in a statistical sense.

In Figure 4 we plot the distributions $p(s)$, normalized to $f_{\text{disk}}/f_{\text{bar}}$, for all galaxies in our sample (hatched areas). In addition we plot $p(s)$ of equation (11) with $\mu = 1.25$ (the median value found by B00) and normalized to unity (solid lines). This distribution is to represent the AMD of the *total* baryonic mass. Then, under the standard assumption that baryons conserve their specific angular momentum, the

difference between the two distributions describes the AMD of the baryonic material that did not make it into the disk.

The first characteristic to note from Figure 4 is that the area under the hatched curves is much smaller than that under the solid lines, reflecting the fact that f_{disk} is significantly smaller than the Universal baryon fraction f_{bar} . Secondly, in all cases $p(s)$ of the total baryonic matter extends to much higher specific angular momenta. This indicates that its ratio $j_{\text{max}}/j_{\text{tot}}$ is larger than that of the disk material (cf. lower right panel of Figure 3), and implies that none of the baryonic material with the highest specific angular momentum has made it into the disk component. Finally, the difference between $p(s)$ of the total baryonic mass and that of the disk mass is largest for small s .

We can thus conclude that if the assumptions made, and which reflect our standard picture for the formation of disk galaxies, are correct, the combined effects of cooling, feedback, and stripping have to be such that: (i) only a small fraction of the available baryons end up in the disk component, (ii) the total specific angular momentum material of the disk is comparable to that of the total baryonic mass, (iii) none of the highest specific angular momentum material makes it into the disk, and (iv) there is a tendency to preferentially prevent low angular momentum material from ending up in the disk.

4.3 Uncertainties in the angular momentum distributions

Before drawing any conclusions regarding the formation of (dwarf) disk galaxies, it is worthwhile to examine some of the uncertainties in the disk AMDs derived above.

4.3.1 The Mass of the Disk

One potential worry is that we have missed a significant fraction of the actual disk mass. In the discussion above we have focussed on results for $\Upsilon_R = 1.0 (M/L)_\odot$, which, for a Scalo (1986) IMF, yields colors in good agreement with the data (see discussion in BS01). However, internal dust extinction could have reddened the galaxies and/or a large fraction of brown dwarfs could be present. Furthermore, a central concentration of molecular gas could be present, which would add low angular momentum material. These uncertainties in the disk's mass distribution can be modeled by varying Υ_R , either as a constant (mimicking for example the presence of brown dwarfs), or as function of radius (mimicking for example the presence of molecular gas). The freedom in $\Upsilon_R(R)$ is limited by the requirement that the mass model has to yield a reasonable fit to the observed rotation curve. We have performed extensive tests with varying $\Upsilon_R(R)$. Within the restrictions imposed by the rotation curves we find that, although it is possible to bring $p(s)$ of the disk in somewhat better agreement with that of the total baryonic mass, the four characteristics listed above remain. This is illustrated in the upper panels of Figure 5 where we plot $p(s)$ of UGC 12632 for three values of Υ_R (taken to be constant with radius). Even for $\Upsilon_R = 8.0 (M/L)_\odot$, which is the maximum mass-to-light ratio allowed by the observed rotation curve, there is still a pronounced deficit of low-angular momentum material in the disk compared to the total baryonic mass component.

4.3.2 The Size of the Disk

The maximum specific angular momentum of the disk, j_{max} , is directly proportional to the size of the disk r_{max} (rotation curves are generally flat at large radii). As stated in Section 3.3, we assume that r_{max} is equal to the radius out to which HI is detected. Typically, these radii coincide with HI column densities of the order of $\sim 10^{19} \text{cm}^{-2}$. This is close to the column density below which one expects the gas to be ionized by the cosmic background flux of ionizing photons (e.g., Sunyaev 1969; Maloney 1993). Therefore, it might well be that the actual gas disk extends significantly beyond the r_{max} adopted here. If we make the assumption that this gas follows the same surface density profile as the HI we can compute the total disk mass missed by integrating equation (13) out to infinity, and comparing that to the total gas mass inside r_{max} . We find that for all galaxies in our sample the gas at radii beyond r_{max} does not contribute more than 0.5 percent of the total disk mass. Thus, whereas the uncertain extent of the disk can imply values of j_{max} that are significantly underestimated, this does not influence our estimates of j_{tot} . For instance, if the actual size of the disks is about 1.4 times r_{max} , the mean of ζ would be in much better agreement with the expected mean for dark matter haloes (lower right panel of Figure 3). Also, the thick curves in Figure 1 would shift to the right by about the same factor, bringing them in somewhat better agreement with the AMDs of B00. However, Figures 2 and 4 would remain virtually unchanged, and except for aspect (iii), the main problems outlined above thus remain.

4.3.3 Asymmetric Drift

Another problem with the AMDs derived in Section 3 is related to the fact that we have assumed that the stars move on purely circular orbits. In reality, however, stars have a non-zero asymmetric drift, and we have thus overestimated the angular momentum of the stellar component. In order to assess the importance of asymmetric drift we perform the following test. We define a free parameter η that describes the (constant) ratio between the true rotation velocity of the stars and the local circular velocity[†]. In the lower three panels of Figure 5 we plot $p(s)$ of UGC 12632 for $\Upsilon_R = 1.0 (M/L)_\odot$ and three different values of η : 0.2, 0.6, and 1.0 (i.e., no asymmetric drift). Only for $\eta \lesssim 0.3$ do we find a discernibly different AMD. Typical asymmetric drifts correspond to values of η much closer to unity, and we therefore conclude that our assumption that $\eta = 1.0$ does not significantly influence our results. This can also be understood directly from the high gas mass fractions found for the dwarf galaxies in our sample. With $0.4 \lesssim f_{\text{gas}} \lesssim 0.9$ the disk mass, and thus the AMD, of our dwarf galaxies is generally dominated by the gas. A small shift of the angular momentum distribution of the stars relative to the gas therefore does not significantly influence the total AMD.

[†] With this definition the asymmetric drift velocity is given by $v_a(r) = (1 - \eta) V_c(r)$.

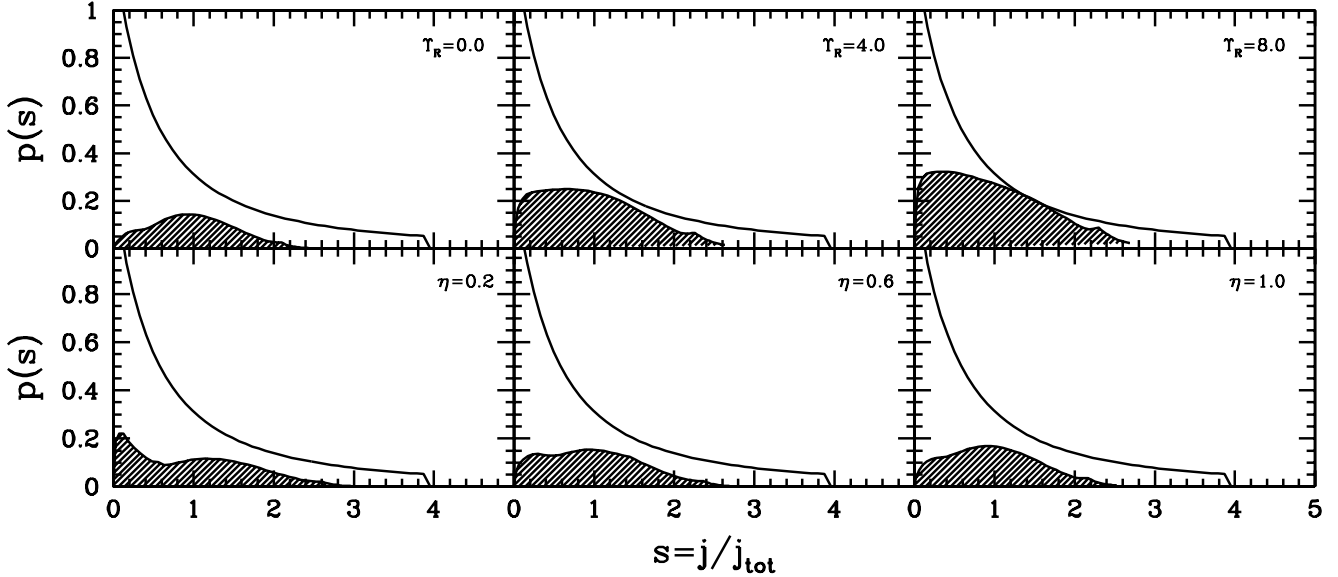


Figure 5. The influence of mass-to-light ratio and asymmetric drift on the AMD of UGC 12632. The upper panels plot $p(s)$ of UGC 12632 for three different values of the stellar mass-to-light ratio (as indicated in each panel). Since the stellar disk is more centrally concentrated than the HI component, increasing Υ_R preferentially increases the disk mass fraction at low angular momentum. However, even for $\Upsilon_R = 8.0 (M/L)_\odot$, the maximum mass-to-light ratio allowed by the rotation curve, a clear deficit at low s remains. The lower panels plot $p(s)$ but now for three different values of η (as indicated in each panel), defined as the ratio of the rotation velocity of the stars to the circular velocity (η is thus a measure of the asymmetric drift). Only for the extreme asymmetric drift corrections with $\eta = 0.2$, does the AMD of UGC 12632 change its characteristic shape. The solid lines are as in Figure 4.

4.3.4 Adiabatic Contraction

In the mass modelling used to fit the observed rotation curves we have made the assumption that the density distribution of the dark matter halo is modified by adiabatic contraction. Since the assumptions underlying the method used (i.e., sphericity, adiabatic invariance) are not necessarily accurate it is worthwhile to examine what effect this adiabatic contraction has on our results. To test this we have reanalyzed all data without any correction for adiabatic contraction. The effects, however, are negligible. Typically one finds values of c_{vir} that are slightly larger (the dark matter halo now needs to be more centrally concentrated in order to fit the observed rotation curve), but the actual AMDs remain virtually unchanged. One parameter that is directly influenced by the change in c_{vir} is the spin parameter λ (equation [5]), but even here the differences are small (less than 5 percent).

Thus, despite considerable freedom in the stellar mass-to-light ratios, the sizes of the disks, and the asymmetric drift corrections, we conclude that the characteristics of the AMDs of disks outlined above are robust. As for the parameters listed in Table 2: f_{gas} , λ_{disk} and j_{tot} are very robust, j_{max} may be significantly underestimated, and the uncertainties on c_{vir} , V_{vir} , and f_{disk} are strongly correlated and discussed in more detail in BS01. Typically, lowering V_{vir} implies larger c_{vir} and f_{disk} . This, through equation (5) results in a slightly larger λ_{disk} . As long as the quality of the rotation curve fit remains similar, the total specific angular momentum, however, remains virtually unchanged. This implies that of the four main characteristics listed in Section 4.2 above, only (iii) is somewhat questionable as it is directly related to the assumed size of the disk.

4.4 Cooling, stripping, feedback & viscosity

If cooling in small mass haloes is very inefficient, it might explain aspects (i) and (iii). After all, cooling is an inside out process, and the highest angular momentum material resides in the outskirts of the haloes. However, as already mentioned in Section 4.1, this picture is inconsistent with (ii), as one would expect λ_{disk} to be much smaller than the spin parameter of the dark matter haloes, and it does not explain aspect (iv). Furthermore, cooling is supposed to be extremely efficient in dense low mass haloes, and one typically expects the vast majority of the baryons in dwarf galaxies to have cooled by the present time. Tidal stripping has virtually the same effects as inefficient cooling; stripping is most efficient near the outskirts of the haloes, and thus might explain both (i) and (iii). However, as with cooling, stripping is inconsistent with both (ii) and (iv).

The problem with feedback as the dominant cause for the AMDs observed is that one would expect a relatively strong correlation between f_{disk} and V_{vir} . After all, the efficiency for blowing a galactic wind should be inversely proportional to the square of the galaxy's escape velocity, which in turn is proportional to V_{vir} . However, the correlation between f_{disk} and V_{vir} has a Spearman rank coefficient of $r_s = -0.411$ and thus seems to indicate an *anti*-correlation (although with a probability of $p_s = 0.14$ this is not significant). Furthermore, as shown by van den Bosch (2001), a simple model for supernovae induced galactic winds does not reveal any tendency to preferentially expel the low angular momentum material as required.

One possibility is that one of the standard assumptions is wrong and that baryons do not conserve their specific angular momentum. However, given that disks have the same

distribution of j_{tot} as the dark matter haloes implies that one can only consider a scenario in which the specific angular momentum of the baryons is redistributed. However, the natural mechanism for angular momentum redistribution, viscosity, transports low angular momentum inwards and high angular momentum material outwards. Therefore, any viscosity present in the disk will only aggravate the disagreement at low and high s between the AMDs of the disk and the total baryonic matter.

4.5 The nature of dark matter

One interesting interpretation of the large differences between the AMDs of disks and cold dark matter haloes found might be that dark matter is not cold. Recently, several studies have focussed on warm and self-interacting dark matter (hereafter WDM and SIDM, respectively) scenarios, and have shown that this results in dark matter haloes with constant density cores and with less substructure (e.g., Spergel & Steinhardt 2000; Burkert 2000a; Colín, Avila-Reese & Valenzuela 2000; Bode, Ostriker & Turok 2000; Davé et al. 2001; Kochanek & White 2000; Moore et al. 2000; Yoshida et al. 2000a,b). Not only might this solve the angular momentum catastrophe mentioned in Section 1 (Sommer-Larsen & Dolgov 2001), it might also alleviate the potential problems with the rotation curves of dwarf and low surface brightness galaxies (Flores & Primack 1994; Moore 1994; Burkert 1995; McGaugh & de Blok 1998; van den Bosch et al. 2000; van den Bosch & Swaters 2001) and with the abundance of satellite galaxies (Kauffmann, White & Guiderdoni 1993; Moore et al. 1999; Klypin et al. 1999). It would be worthwhile to examine to what extent these differences in halo structure result in AMDs that are different from those of CDM haloes. For instance, Moore et al. (2000) have pointed out that the central regions of SIDM haloes are rotationally supported, implying AMDs with less low angular momentum material compared to CDM haloes.. Detailed high resolution N -body simulations of structure formation in WDM and SIDM cosmologies are required to test whether a modification of the nature of dark matter brings the AMDs of disks and dark matter haloes in better agreement.

4.6 Decoupling the baryons from the dark matter

Probably the most likely conclusion from our results is that the standard assumption that baryons and dark matter have the same AMD is incorrect. Since dark and baryonic matter should in principle experience the same cosmological torques, we thus need a mechanism to somehow decouple the baryonic mass component from that of the dark matter. One such mechanism, suggested by Hogan (1979), is Compton drag on the background radiation. This causes the gas to be frozen into the comoving frame such that it experiences no tidal torques. However, this mechanism is only efficient at very high redshifts, and will cause the baryons to have less specific angular momentum than the dark matter. This is inconsistent with what is required, since, as shown by Burkert (2000b), the strong correlation between f_{disk} and λ_{disk} found requires a mechanism that can actually spin-up the baryons relative to the dark matter.

A more plausible mechanism might be to resort to feed-

back from early structure formation which stirs up the baryonic component resulting in a density distribution that is quite distinct from that of the dark matter. Subsequent torques will then be different for the two mass components, causing a decoupling of their angular momentum distributions. Furthermore, it is important to realize that because of the dissipative nature of the baryonic matter, angular momentum redistribution in merging systems will be quite different for baryonic and dark matter. High resolution hydro-dynamical simulations should be useful to investigate whether the AMDs of baryons and dark matter are similar (as usually assumed), or whether the processes mentioned above cause a decoupling that bring the AMDs of the baryonic component in better agreement with those of disk galaxies.

5 SUMMARY

In the standard picture of structure formation the angular momentum of protogalaxies originates from cosmological torques. Since dark and baryonic matter experience the same tidal forces, it is expected that both mass components end up with the same distribution of specific angular momentum. In a recent paper Bullock et al. (2000) determined the AMDs of dark matter haloes in a Λ CDM cosmology. If our picture of disk formation is correct, we thus expect disks to be born out of similar distributions. A comparison of the AMDs of disks with those of dark matter haloes thus yields important insights into the formation mechanism of galaxies, and may be used to test our standard picture of disk formation.

In this paper we have computed the AMDs of a sample of 14 dwarf galaxies with observed HI rotation curves. These rotation curves have been analyzed in detail by van den Bosch & Swaters (2001), who found them to be in good agreement with Λ CDM predictions. A comparison with the AMDs of dark matter haloes obtained by B00 reveals the following:

- The ratios of disk mass to total virial mass, f_{disk} , inferred from mass models fitted to the observed rotation curves, are much smaller than the Universal baryon fraction f_{bar} for currently popular cosmologies. This indicates that large fractions of baryonic mass have either been prevented from cooling, or have been removed from the disk or halo by either feedback or stripping mechanisms.
- The distribution of λ_{disk} is in good agreement with the distribution of halo spin parameters. This suggests that disks have the same *total* specific angular momentum as dark matter haloes.
- The disk mass fractions f_{disk} are strongly correlated with the disk's spin parameter λ_{disk} .
- The distribution of $\zeta = j_{\text{tot}}/j_{\text{max}}$ of disks is narrower than $p(\zeta)$ of dark matter haloes, and with a mean that is significantly higher. This implies that the AMDs of haloes have more extended tails to high specific angular momentum.
- The normalized angular momentum distributions of (low mass) disk galaxies are clearly distinct from those of dark matter haloes. The latter have AMDs that extent to higher specific angular momentum, and with much more mass at low angular momentum.

Despite uncertainties in the disk's density distribution, related to the unknown mass-to-light ratio and the unknown amount of molecular gas, these results are robust, and confirm recent findings of Navarro & Steinmetz (2000) that apparently disks form out of a small fraction of the available baryonic mass, but yet manage to tap most of the available specific angular momentum.

Understanding these findings within the standard framework of disk formation is challenging. Neither the main mechanisms that lead to small values of f_{disk} , i.e., feedback, stripping or cooling, nor viscous processes that redistribute specific angular momentum, seem able to provide a meaningful explanation. Somehow these results seem to imply that the baryonic mass components out of which disk galaxies form through cooling have angular momentum distributions that are clearly distinct from those found by B00. This implies either that some mechanism decoupled the baryons from the dark matter during the early stages of the formation of galaxies (during which they acquire angular momentum from cosmological torques), or that the distributions found by B00 are poor descriptions of the actual AMDs of dark matter haloes (perhaps reflecting a different nature of the dark matter). It is clear that without a proper understanding of (the origin of) the angular momentum distribution of the baryonic mass component of protogalaxies our picture of the formation of disk galaxies is incomplete.

ACKNOWLEDGEMENTS

We are grateful to Tom Abel, Houjun Mo, Yi-Peng Jing and Simon White for stimulating discussions. FB thanks the hospitality of the MPIA in Heidelberg during his visit that started the work presented here.

REFERENCES

- Avila-Reese V., Firmani C., 2000, *RevMexAA*, 36, 23
Bahcall N.A., Fan X., 1998, *ApJ*, 504, 1
Barnes J.E., White S.D.M., 1984, *MNRAS*, 211, 753
Barnes J.E., Efstathiou G., 1987, *ApJ*, 319, 575
Bell E.F., de Jong R.S., 2001, *ApJ*, 550, 212
Blumenthal G.R., Faber S.M., Flores R., Primack J.R., 1986, *ApJ*, 301, 27
Bode P., Ostriker J.P., Turok N., 2000, preprint (astro-ph/0010389)
Bryan G., Norman M., 1998, *ApJ*, 495, 80
Buchalter A., Jimenez R., Kamionkowski M., 2001, *MNRAS*, 322, 43
Bullock J.S., Dekel A., Kolatt T.S., Kravtsov A.V., Klypin A.A., Porciani C., Primack J.R., 2000, preprint (astro-ph/0011001), B00
Bullock J.S., Kolatt T.S., Sigad Y., Somerville R.S., Kravtsov A.V., Klypin A.A., Primack J.R., Dekel A., 2001, *MNRAS*, 321, 559
Burkert A., 1995, *ApJ*, 447, L25
Burkert A., 2000a, *ApJ*, 534, L143
Burkert A., 2000b, preprint (astro-ph/0007047)
Catelan P., Theuns T., 1996, *MNRAS*, 282, 436
Cole S., Lacey S., 1996, *A&A*, 281, 716
Colín P., Avila-Reese V., Valenzuela O., 2000, *ApJ*, 542, 622
Dalcanton J.J., Spergel D.N., Summers F.J., 1997, *ApJ*, 482, 659
Davé R., Spergel D.N., Steinhardt P.J., Wandelt B.D., 2001, *ApJ*, 547, 574
de Bernardis P. et al., 2000, *Nature*, 404, 955
Doroshkevich A. G., 1970, *Astrofizika*, 6, 581
Efstathiou G., 2000, *MNRAS*, 317, 697
Eke V.R., Cole S., Frenk C.S., 1996, *MNRAS*, 282, 263
Fall S.M., Efstathiou G., 1980, *MNRAS*, 193, 189
Firmani C., Avila-Reese V., 2000, *MNRAS*, 315, 457
Flores R., Primack J.R., Blumenthal G.R., Faber S.M., 1993, *ApJ*, 412, 443
Flores R., Primack J.R., 1994, *ApJ*, 427, L1
Garnavich P.M. et al., 1998, *ApJ*, 509, 74
Heavens A.F., Jimenez R., 1999, *MNRAS*, 305, 770
Hogan C.J., 1979, *MNRAS*, 188, 781
Hoyle F., 1953, *ApJ*, 118, 513
Jimenez R., Padoan P., Matteucci F., Heavens A.F., 1998, *MNRAS*, 296, 1089
Kauffmann G., 1996, *MNRAS*, 281, 475
Kauffmann G., White S.D.M., Guiderdoni B., 1993, *MNRAS*, 264, 201
Klypin A.A., Kravtsov A.V., Valenzuela O., Prada F., 1999, *ApJ*, 522, 82
Kochanek C.S., White M., 2000, *ApJ*, 543, 514
Maloney P., 1993, *ApJ*, 414, 41
McGaugh S.S., de Blok W.J.G. 1998, *ApJ*, 499, 41
Mo H.J., Mao S., White S.D.M., 1998, *MNRAS*, 295, 319
Moore B., 1994, *Nature*, 370, 629
Moore B., Ghigna S., Governato F., Lake G., Quinn T., Stadel J., Tozzi P., 1999, *ApJ*, 524, L19
Moore B., Gelato S., Jenkins A., Pearce F.R., Quilis V., 2000, *ApJ*, 535, L21
Natarajan P., 1999, *ApJ*, 512, 105
Navarro J.F., Benz W., 1991, *ApJ*, 380, 320
Navarro J.F., Frenk C.S., White S.D.M., 1996, *ApJ*, 462, 563
Navarro J.F., Frenk C.S., White S.D.M., 1997, *ApJ*, 490, 493
Navarro J.F., Steinmetz M., 2000, *ApJ*, 538, 477
Peebles P.J.E., 1969, *ApJ*, 155, 393
Perlmutter S. et al., 1998, *Nature*, 391, 51
Riess A.G. et al., 1998, *AJ*, 116, 1009
Ryden B.S., 1988, *ApJ*, 329, 589
Scalo J.N., 1986, *Fundam. Cosmic Phys.*, 11, 1
Sommer-Larsen J., Dolgov A., 2001, *ApJ*, 551, 608
Spergel D.N., Steinhardt P.J., 2000, *Phys. Rev. Lett.*, 84, 17
Steinmetz M., Navarro J.F., 1999, *ApJ*, 513, 555
Sugerman B., Summers F.J., Kamionkowski M., 2000, *MNRAS*, 311, 762
Sunyaev R.A., 1969, *Astrophys. Letters*, 3, 33
Swaters R.A., 1999, PhD Thesis, University of Groningen, The Netherlands
Tytler D., Burles S., Lu L., Fan X.-M., Wolfe A., Savage B., 1999, *AJ*, 117, 63
van den Bosch F.C., 1998, *ApJ*, 507, 601
van den Bosch F.C., 2000, *ApJ*, 530, 177
van den Bosch F.C., 2001, *MNRAS*, submitted
van den Bosch F.C., Dalcanton J.J., 2000, *ApJ*, 534, 146
van den Bosch F.C., Robertson B.E., Dalcanton J.J., de Blok W.J.G., 2000, *AJ*, 119, 1579
van den Bosch F.C., Swaters R.A. 2001, *MNRAS*, in press (astro-ph/0006048)
Warren M.S., Quinn P.J., Salmon J.K., Zurek W.H., 1992, *ApJ*, 399, 405
White S.D.M., 1984, *ApJ*, 286, 38
White S.D.M., Navarro J.F., 1993, *MNRAS*, 265, 271
Yoshida N., Springel V., White S.D.M., Tormen G., 2000a, *ApJ*, 535, L103
Yoshida N., Springel V., White S.D.M., Tormen G., 2000b, *ApJ*, 544, L87
Zhang B., Wyse R.F.G., 2000, *MNRAS*, 313, 310
Zurek W.H., Quinn P.J., Salmon J.K., 1988, *ApJ*, 330, 519